Journal of Cerebral Blood Flow & Metabolism (2008) 28, 1275–1284

www.jcbfm.com

Acute functional recovery of cerebral blood flow after forebrain ischemia in rat

Chao Zhou[1], Tomokazu Shimazu[2], Turgut Durduran[1,3], Janos Luckl[2], Daniel Y Kimberg[2], Guoqiang Yu[1,4], Xiao-Han Chen[5], John A. Detre[2,3], Arjun G Yodh[1] and Joel H Greenberg[2]

[1]*Department of Physics and Astronomy, University of Pennsylvania, Philadelphia, Pennsylvania, USA;* [2]*Department of Neurology, University of Pennsylvania, Philadelphia, Pennsylvania, USA;* [3]*Department of Radiology, University of Pennsylvania, Philadelphia, Pennsylvania, USA;* [4]*Wenner-Gren Research Lab, Center for Biomedical Engineering, University of Kentucky, Lexington, Kentucky, USA;* [5]*Department of Neurosurgery, University of Pennsylvania, Philadelphia, Pennsylvania, USA*

After complete cerebral ischemia, the postischemic blood flow response to functional activation is severely attenuated for several hours. However, little is known about the spatial and temporal extent of the blood flow response in the acute postischemic period after incomplete cerebral ischemia. To investigate the relative cerebral blood flow (rCBF) response in the somatosensory cortex of rat to controlled vibrissae stimulation after transient incomplete ischemia (15-min bilateral common carotid artery occlusion + hypotension), we employed laser speckle imaging combined with statistical parametric mapping. We found that the ischemic insult had a significant impact on the baseline blood flow ($P < 0.005$) and the activation area in response to functional stimulation was significantly reduced after ischemia ($P < 0.005$). The maximum rCBF response in the activation area determined from the statistical analysis did not change significantly up to 3 h after ischemia ($P > 0.1$). However, the time when rCBF response reached its maximum was significantly delayed ($P < 0.0001$) from 2.4 ± 0.2 secs before ischemia to 3.6 ± 0.1 secs at 20 mins into reperfusion ($P < 0.001$); the delay was reduced gradually to 2.9 ± 0.2 secs after 3 h, which was still significantly greater than that observed before the insult ($P = 0.04$).
Journal of Cerebral Blood Flow & Metabolism (2008) **28,** 1275–1284; doi:10.1038/jcbfm.2008.21; published online 2 April 2008

Keywords: cerebral blood flow; cerebral ischemia; functional activation; functional recovery; laser speckle imaging; statistical parametric map

Introduction

There has been considerable interest in the ability of the cerebrovasculature to respond to functional stimulation after a period of transient cerebral ischemia (Schmitz *et al*, 1997, 1998; Ueki *et al*, 1988; Ances *et al*, 2000; Dijkhuizen *et al*, 2003), which may provide a window into the eventual fate of the tissue. Better characterization of these responses after ischemia could also be important for interpreting studies of functional reorganization after ischemic injury. After cardiac arrest, during which cerebral blood flow (CBF) is reduced to zero, magnetic resonance (MR)-based perfusion imaging shows a lack of hemodynamic response to electrical forepaw stimulation 1 h after resuscitation, and only a minimal response after 3 h (Schmitz *et al*, 1998). During the first 24 h of reperfusion, MR-based signals of functional recovery return, with the perfusion-weighted response to stimulation recovering more slowly than does the blood oxygen level-dependent measurement. If both vertebral and carotid arteries are occluded for 30 mins, also producing negligible blood flow in the somatosensory cortex, the tissue loses its ability to respond to electrical forepaw stimulation even after 3 h of recirculation (Ueki *et al*, 1988). There are significant differences, however, between complete ischemia (no blood flow) and severe incomplete ischemia (CBF less than 10% of normal) (Benzi *et al*, 1978; Dietrich *et al*, 1987; Steen *et al*, 1979). During incomplete ischemia, such as temporary middle cerebral artery occlusion, hemodynamic response in the somatosensory cortex to electrical stimulation of the contralateral forepaw is significantly attenuated 1 day after the occlusion and

Correspondence: Dr JH Greenberg, Department of Neurology, University of Pennsylvania, 415 Stemmler Hall, 3450 Hamilton Walk, Philadelphia, PA 19104, USA.
E-mail: joel@mail.med.upenn.edu
This work was supported by US Public Health Service NIH Grants NS-33785 (JHG) and HL-077699 (AGY).
Received 25 October 2007; revised 29 January 2008; accepted 28 February 2008; published online 2 April 2008

is not normalized until approximately 2 weeks (Dijkhuizen *et al*, 2003). There is no information, however, concerning the ability of the cerebrovasculature to respond to functional stimulation very acutely after incomplete ischemia, and, in particular, whether the spatial extent of the activation is altered by the ischemic insult.

Laser speckle imaging (LSI; Briers, 2001; Dunn *et al*, 2001) provides two-dimensional blood flow maps with high spatial and temporal resolution. The LSI technique shares the same basic physical picture with the laser-Doppler perfusion technique: scattered laser light with different pathlength produces a random interference pattern known as speckle, whose fluctuations contain information about motions of particles in the underlying medium. A variety of methods (Briers, 2001) use this effect for tissue studies, including laser-Doppler flowmetry (Bonner and Nossal, 1990) and diffuse correlation spectroscopy (Boas and Yodh, 1997). Recently, LSI has been widely used to measure CBF during functional stimulation and physiologic perturbation in rodent and cat cortex (Dunn *et al*, 2001; Durduran *et al*, 2004; Weber *et al*, 2004; Ayata *et al*, 2004; Shin *et al*, 2006; Strong *et al*, 2006).

We used LSI to investigate the near-surface activation flow coupling after electrical somatosensory stimulation of forepaw and hindpaw in rat (Durduran *et al*, 2004). Using high-resolution temporal (5 Hz) and spatial sampling (32 μm), the effects of stimulus amplitude and duration were investigated. Basic functional mapping was shown by separating the activation after forepaw and hindpaw stimulation, and correlation coefficient images were used to characterize the spatial extent of the activation. However, the regions of interest (ROIs) were determined from the rescaled correlation coefficient images by setting an arbitrary threshold or by using a full-width at half-maximum approach (Durduran *et al*, 2004; Weber *et al*, 2004; Dunn *et al*, 2005). This makes it difficult to compare the activation areas under different physiologic conditions, such as after cerebral ischemia, as the maximum may also be a variable. Conversely, statistical parametric mapping (SPM), which is widely used in the functional MRI community (Friston *et al*, 1995; Worsley and Friston, 1995), enables statistical comparison and interpretation of activation under various physiologic conditions. To this end, a modified general linear model (GLM) (Worsley and Friston, 1995) was employed to construct robust statistical parametric maps for spatially extended processes in the presence of temporal autocorrelation. We used the SPM approach with LSI data to examine the relative cerebral blood flow (rCBF) response in the somatosensory cortex of rat to controlled vibrissae stimulation after temporary incomplete ischemia. We found that the activation area and temporal response to stimulation were altered acutely after severe incomplete cerebral ischemia, whereas the maximum CBF response to functional stimulation was preserved.

Materials and methods

Surgical Preparation

Animal procedures were in accordance with the guidelines established by the National Institutes of Health and were approved by the Institutional Animal Care and Use Committee at the University of Pennsylvania. Studies were undertaken in 10 male Sprague–Dawley rats ($N = 10$, 325 ± 39 g; Charles River, Wilmington, MA, USA), which had free access to food and water. They were anesthetized with halothane in a bell jar, tracheally intubated, and mechanically ventilated with 1.0% halothane in 30% O_2 balanced with 70% N_2O. One femoral artery was cannulated for blood pressure monitoring and blood gas sampling, and a catheter was placed into the other femoral artery for blood withdrawal during the production of hypotension. Body temperature was maintained at $37.5^{\circ}C \pm 0.2^{\circ}C$ and $PaCO_2$ levels were kept between 35 and 45 mm Hg by adjusting the respirator based on periodic arterial blood gas sampling. An 8 mm diameter region over the right whisker barrel somatosensory area centered at 6 mm lateral and 2 mm posterior to the bregma was thinned using a saline-cooled dental drill. After the surgical preparation, the animals were administered 60 mg/kg of α-chloralose intraperitoneally and halothane was discontinued. Hourly supplemental doses of α-chloralose (30 mg/kg intraperitoneally) were administered and the animals were maintained on 30% O_2 balanced with 70% N_2. All whiskers except for B1-3, C1-3, and D1-3 on the left were cut at the level of the skin to prevent accidental stimulation.

Transient forebrain ischemia was produced by bilateral carotid arterial occlusion (2VO) with controlled hypotension (Nordström and Siesjö, 1978; Smith *et al*, 1984). Loose snares were placed around both carotid arteries and mean arterial blood pressure was lowered to 45 to 50 mm Hg by slowly withdrawing blood from the femoral arterial catheter into a heparinized syringe. The snares were then tightened and the mean arterial blood pressure was maintained at this level for 15 mins, at which time the snares were removed and the withdrawn blood was returned to the animal over a period of 5 mins.

A group of control rats were prepared similar to the animals with transient forebrain ischemia, except that the carotid artery snares were not tightened and blood was not withdrawn from the arterial catheter ($N = 6$).

Stimulus Presentation and Experiment Protocol

The experiment protocol consisted of 20 secs of image acquisition. After a 5-sec data collection (no stimulus) procedure, the vibrissae were stimulated for 3 secs; data were taken poststimulus for 12 secs. Stimulation consisted of mechanical stroking of the left vibrissa (B1-3, C1-3, and D1-3) with a solenoid driven in the rostral–caudal direction at 5 Hz. This protocol was repeated 10 times with 40 secs of no data acquisition (or stimulation) between runs. Thus, the vibrissae were stimulated for only 3 secs/min. Vibrissae stimulations (and LSI data acquisitions) were performed before ischemia and at 20 mins, 30 mins,

1 h, 2 h, and 3 h after reperfusion. Animals were killed after the 3 h measurement with an overdose of a barbiturate (150 mg/kg) and the brain removed from the skull. The cortices were carefully removed from the remainder of the brain, flattened between two silicone-coated glass slides separated by 4 mm spacers, and frozen in isopentane cooled to −30°C. The right cortex was mounted in a cryostat (Bright Instrument Company Ltd, Huntingdon, England) and, after temperature equilibration, was sectioned tangential to the cortical surface. Sequential sections were stained for cytochrome oxidase, as described previously (Sohn *et al*, 1999). Images from the cytochrome oxidase staining, which map the walls of the vibrissae barrels, were coregistered with the LSI images using a warping technique described by Bookstein (1989).

Laser Speckle Imaging

The basics of the LSI technique have been described in detail earlier (Goodman, 1985; Briers, 2001; Dunn *et al*, 2001; Bandyopadhyay *et al*, 2005). Briefly, when coherent laser light is shone on a turbid medium, such as biologic tissue, photons traveling from different scattering paths form random speckle patterns on the surface of the medium, which can be captured by a CCD (charge-coupled device) camera. The intensity of each speckle fluctuates if the scattering particles are in motion inside the tissue. Within a given exposure time, speckle visibility of the region with faster particle movements is lower than the region with slower particle movements, because of stronger blurring of the speckle patterns. The speckle visibility at each position can be quantified as speckle contrast (C) by calculating the ratio of s.d. (σ) and the mean ($\langle I \rangle$) of the intensity within a square window, for example, 5×5 pixels. The correlation time (τ_c) of the tissue, which is inversely proportional to the mean velocity of the scattering particles (Ayata *et al*, 2004), is related to the speckle contrast by a simple formula (Goodman, 1985; Bandyopadhyay *et al*, 2005),

$$C = \frac{\sigma}{\langle I \rangle} = \left[\beta \frac{\tau_c^2}{2T^2} \left(e^{-2\frac{T}{\tau_c}} - 1 + 2\frac{T}{\tau_c} \right) \right]^{\frac{1}{2}} \quad (1)$$

where T is the camera exposure time, and the coherence factor β depends on the size ratio of the speckle and the CCD pixel. Note that equation (1) describes the relationship between speckle contrast and correlation time more accurately (Bandyopadhyay *et al*, 2005; Wang *et al*, 2007), compared with the formula widely used in laser speckle literature (Dunn *et al*, 2001; Durduran *et al*, 2004; Ayata *et al*, 2004). However, no significant discrepancies were found between the two formulae, when used for relative blood flow measurements (Wang *et al*, 2007).

The LSI device and scanning procedure used in this study have been described in detail earlier (Durduran *et al*, 2004). A collimated diode laser (Hitachi, HL 785 1G, 785 nm, 50 mW; Thorlabs, Newton, NJ, USA) was used to illuminate the cerebral cortex through the thinned window on the skull at 30 to 40° from vertical. A 60 mm lens (AF Micro-Nikkor 60 mm f/2.8D; Nikon, NY, USA) was used for the imaging and the aperture was adjusted to match the speckle size to the CCD pixel dimensions ($6.45\,\mu m \times 6.45\,\mu m$) (Dunn *et al*, 2001; Durduran *et al*, 2004). Thus, β was assumed to be unity in the following calculations. Images were recorded at 5 Hz with a cooled CCD camera (Retiga 1350EX, QImaging, Surrey, BC, Canada) using commercial imaging software (StreamPix, NorPix, Montreal, QC, Canada). Both the camera and the mechanical stimulator were externally triggered for the coregistration of stimulation and data acquisition.

Equation (1) was used to extract $1/\tau_c$ from the speckle contrast on each pixel as the index for CBF values. We have noticed that $1/\tau_c$ is not zero when tissue perfusion is zero (post mortem), an observation also made by other laboratories (Ayata *et al*, 2004; Strong *et al*, 2006). This so-called 'biological zero' mainly corresponds to the random motion of scatterers in the tissue and is extensively discussed in the laser-Doppler literature (Kernick *et al*, 1999). In a separate group of animals without ischemic insults ($N = 6$), laser speckle images were obtained before (baseline) and after killing (dead), to quantify the values for biological zero. We found that biological zero expressed in percentage (post-mortem flow/baseline flow) showed more consistent results across animals compared with the absolute $1/\tau_c$ values. An average of 11.7% ± 2.4% (mean ± s.e.m.) was obtained from the six animals and was used to correct for CBF values throughout the analysis in the ischemic group.

To reduce the data to be processed to a manageable size, the images were smoothed using a bi-cubic interpolation method by 5×5, thereby reducing the spatial resolution to $32.25\,\mu m$. Relative changes in CBF because of vibrissal stimulation (rCBF) were obtained by dividing each image by the average baseline image obtained during the 5 secs before the start of the stimulus. The data collected during the repeat stimulations were collapsed by aligning time points and calculating the mean of the images. Changes in blood flow during the ischemic and reperfusion periods were calculated by dividing each image by the average of images obtained before the onset of ischemia.

Data Analysis

A modified GLM (Worsley and Friston, 1995) was employed to estimate the spatial extent of the activation using a free software package VoxBo (http://www.voxbo.org). Basically, the GLM treats a series of measurement data $\boldsymbol{X}$ as the linear combination of a set of independent covariates,

$$\boldsymbol{X} = \boldsymbol{G}\gamma + \boldsymbol{e} \quad (2)$$

where the columns of the design matrix (G) are the covariates, the parameter vector γ represents the weights for each covariate, and $\boldsymbol{e}$ is the error term. The modified GLM makes it possible to estimate the parameters and contrast them statistically in the presence of temporal autocorrelation (because of high-frequency noise and low-frequency shifts in the data).

In our study, the rCBF images from individual animals were spatially smoothed with a 5×5 pixel spatial Gaussian filter before they were imported into Voxbo. Covariates of interest represent the contrast of activity at

each second after the onset of stimulation (up to 7 secs), and covariates of no interest were defined as the intercept of each trial. Statistical parametric maps (*t*-statistics) contrast the rCBF response during the time period 2 to 5 secs into stimulation (2, 3, 4, and 5 secs) with baseline. A statistical significance was set to a threshold (e.g., p_{th} = 0.01 or 0.05) and the corresponding Bonferroni-corrected threshold *t*-values were calculated based on the degree of freedom and the number of pixels in the image.

To investigate the spatio-temporal response simultaneously, an ROI was defined independently at each time point (before and after the ischemic insult) for each animal as all pixels with *t*-value above the threshold. The number of pixels within the ROI was used to calculate the 'area of activation,' which was used to quantify the spatial response to the ischemic insult. The temporal changes were reduced to a curve by averaging rCBF over all pixels within the ROI at each time point. Maximum ΔrCBF and the time to reach maximum ΔrCBF were calculated from the curve for the quantification of the temporal responses after the ischemic insult for each animal.

Results from the ischemic and control groups were expressed as mean ± s.e.m. Significant differences between pre- and postischemia were determined with one-way repeated measures ANOVA. When significant differences were found, the Tukey test was used to find at which time point these differences occurred.

Results

Physiologic Variables

The blood gases in the ischemic animals were all within the normal range ($PaCO_2$: 42.7 ± 1.8 mm Hg; PaO_2: 109 ± 4 mm Hg; pH: 7.39 ± 0.02) and were not significantly different during the ischemic and reperfusion periods. The mean arterial blood pressure was 118 ± 3 mm Hg before the generation of hypotension and was reduced to 47.6 ± 1.2 mm Hg during the bleeding phase. After release of the ligatures around the carotid arteries and reinfusion of the shed blood, blood pressure increased to 122 ± 3 mm Hg (Figure 1). The blood gases ($PaCO_2$: 37.7 ± 1.1 mm Hg; PaO_2: 118 ± 7 mm Hg; pH: 7.43 ± 0.02) and blood pressures (117 ± 4 mm Hg) in the control group were very similar to the ischemic animals and did not differ significantly during the course of the study.

Cerebral Blood Flow During Ischemia

When the carotid arteries were ligated and the arterial blood pressure decreased, rCBF in the middle cerebral artery territory decreased rapidly to 6.6% ± 1.8% (N = 10) of baseline within a couple of minutes and remained at that level for 15 mins (Figure 1). On release of the carotid ligatures and reinfusion of the shed blood, rCBF increased to well above the baseline value, peaking at 538% ± 35%, approximately 9 to 10 mins after the end of the ischemic period, before decreasing to close to the baseline level approximately 17 mins after the start of reperfusion.

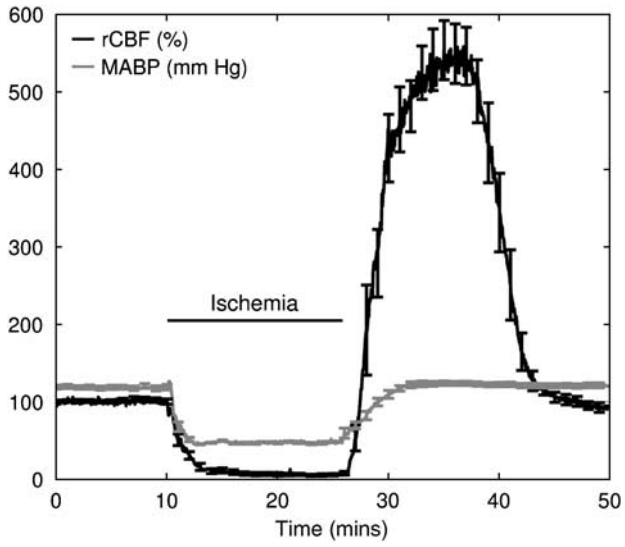

Figure 1 Average relative cerebral blood flow (rCBF) and mean arterial blood pressure (MABP) measured during incomplete ischemia (N = 10).

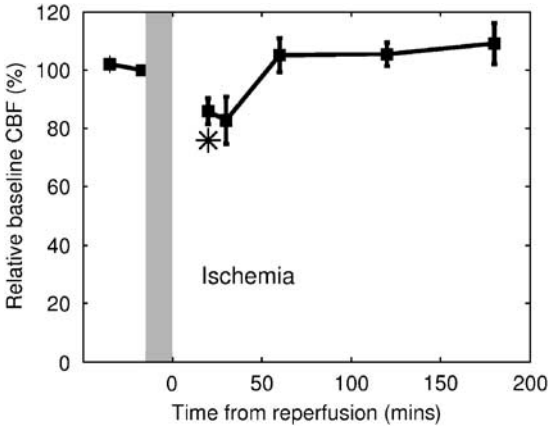

Figure 2 Baseline cerebral blood flow (CBF) changes before and after ischemic insults. Symbols indicate significant difference from preischemic values (P < 0.05).

Baseline Cerebral Blood Flow Variations because of Severe Incomplete Ischemia

The ischemic insult was found to have a significant effect on the baseline CBF (ANOVA, P = 0.004). Figure 2 shows the baseline variations before and after the ischemic insult. Data at different time points were normalized to the baseline values right before ischemia (Figure 1). Twenty minutes after reperfusion, baseline CBF was significantly lower than the preischemic level (86% ± 4%, P = 0.01); although at 30 mins, baseline CBF was also lower

than the preischemic level (83% ± 8%), this difference was not statistically significant ($P = 0.06$). However, baseline CBF returned to the preischemic level 1 h after reperfusion, which indicates a clear recovery of cerebral perfusion.

Functional Responses After Ischemic Insult

Peak ΔrCBF images: Figure 3A shows images of peak ΔrCBF responses to the whisker stimulation from one representative animal before and after the ischemic insult. Images within 2 secs from the peak ΔrCBF changes (see Figure 6B) were averaged for the display at each time point. Outlines of whisker barrels (B1 to D3) from stained brain slices were superimposed on the preischemic ΔrCBF image. In general, blood flow responses covered a larger region on the brain compared with the whisker barrels.

Activation area variations: The amount of tissue that is considered activated by vibrissae stimulation depends on what is used for the threshold of activation. Figures 3B and 3C show the activation area (pseudo-color) superimposed on the vasculature map (black and white) from the same animal described above (Figure 3A). Images from two different threshold levels ($p_{th} = 0.05$ and $p_{th} = 0.01$) are displayed for comparison. Pixels having a *t*-value greater than the corresponding Bonferroni-corrected *t*-threshold are shown in color, with the same threshold *t*-value used for the analysis at different time points before and after ischemia. The activation region appears larger when the threshold is set to 0.05 (Figure 3B), compared with the threshold at 0.01 (Figure 3C). The size of the region is significantly altered by the ischemic insult (ANOVA, $P < 0.005$ for both thresholds). Although the absolute values of the activation area depend on the threshold, the activation area changes similarly during the reperfusion period (Figure 4). Because the temporal changes in the activation area are similar for both thresholds, observed also for other parameters (see Figure 6), henceforth we use $p_{th} = 0.01$ as the threshold for the selection of ROIs. Using this threshold, the activation area was found to be significantly reduced from the preischemic level ($8.5 \pm 1.0\,mm^2$) during the recovery from ischemia

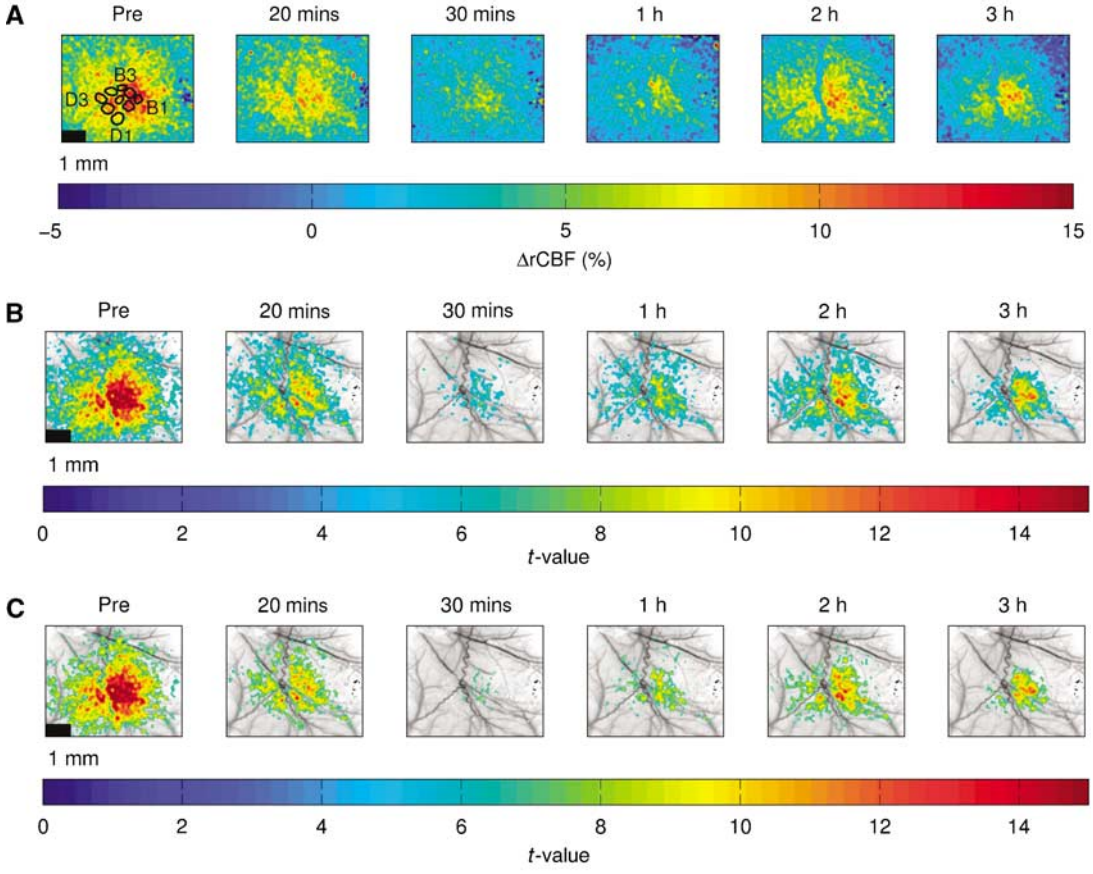

Figure 3 Images from a representative animal showing functional activations before and after ischemic insult. (**A**) Peak ΔrCBF images with whisker barrels superimposed. Blood flow response covers a larger region on the brain compared with the whisker barrels. (**B** and **C**) Statistical parametric maps from the general linear model analysis showing the activation area at different threshold levels; panel B: $p_{th} = 0.05$ and panel C: $p_{th} = 0.01$. Black and white background, vasculature map; pseudo-color foreground, activation area; rCBF, relative cerebral blood flow.

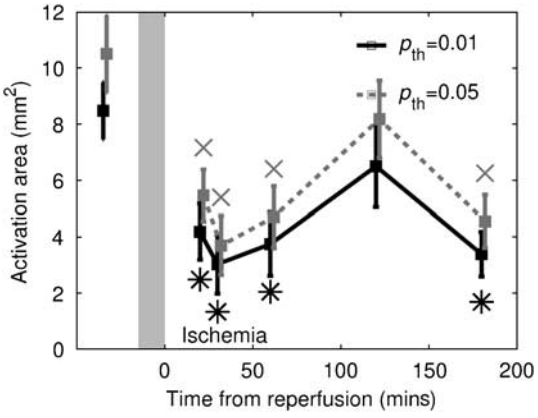

Figure 4 Activation area before and after ischemic insult ($N = 10$). Activation area decreased significantly at 20 mins, 30 mins, 1 h, and 3 h after reperfusion ($P < 0.05$), but no significant decreases were observed at the 2 h time point. Symbols indicate significant difference from preischemic values ($P < 0.05$).

(20 mins: $4.2 \pm 1.0\,mm^2$, $P = 0.009$; 30 mins: $3.0 \pm 1.0\,mm^2$, $P = 0.007$; 1 h: $3.7 \pm 1.1\,mm^2$, $P = 0.02$; 3 h: $3.4 \pm 0.8\,mm^2$, $P = 0.002$). There was no significant reduction in the area of activation 2 h after the end of ischemia.

In the control group, the activation area was $7.3 \pm 0.9\,mm^2$, which neither changed significantly during the course of the various scans ($P = 0.61$) nor was different from the activation area of the ischemia group before ischemia ($P = 0.43$).

ΔrCBF time curves: Before ischemia, blood flow started increasing about 1 sec after the onset of the stimulation and reached its maximum approximately 2.5 secs into the stimulation (Figure 5). Twenty minutes after the ischemic insult, ΔrCBF responded more slowly to the vibrissae stimulation and the maximum ΔrCBF appeared smaller compared with the preischemic response; by 2 h after ischemia, recovery in both amplitude and response time was observed.

Maximum ΔrCBF changes: Statistical analysis showed that the maximum ΔrCBF response to the stimulation was not significantly influenced by the ischemic insult (ANOVA, $P = 0.14$ and 0.18 for $p_{th} = 0.01$ and 0.05, respectively). Before ischemia, the maximum ΔrCBF response to the vibrissae stimulation was $11.1\% \pm 0.9\%$ ($p_{th} = 0.01$; Figure 6A); maximum ΔrCBF slightly decreased to $9.4\% \pm 0.3\%$ approximately 20 mins into reperfusion ($P = 0.07$) and stayed around the preischemic level for the remaining 3 h (30 mins: $9.9\% \pm 0.7\%$, $P = 0.33$; 1 h: $9.8\% \pm 0.7\%$, $P = 0.22$; 2 h: $11.1\% \pm 0.9\%$, $P = 0.98$; 3 h: $11.9\% \pm 0.8\%$, $P = 0.44$). The control animals showed a stable response at all time points from before the sham ischemia ($9.7\% \pm 0.6\%$) to the scan more than 3 h later ($10.3\% \pm 0.6\%$; ANOVA, $P = 0.40$).

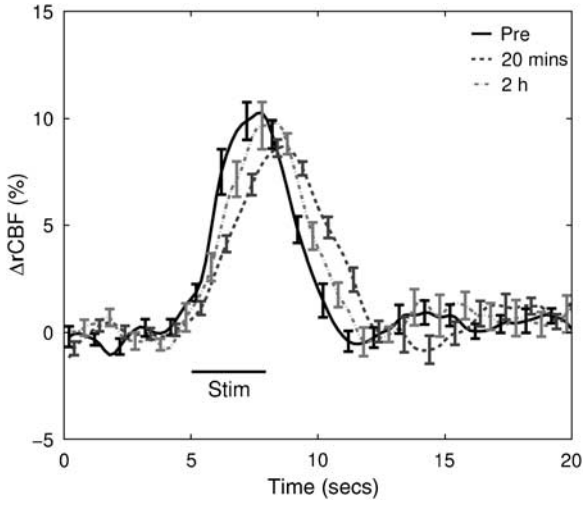

Figure 5 Average ΔrCBF curves in response to stimulation before and after ischemic insult from all animals ($N = 10$). Regions of interest were chosen for each time point based on the general linear model analysis ($p_{th} = 0.01$). rCBF, relative cerebral blood flow.

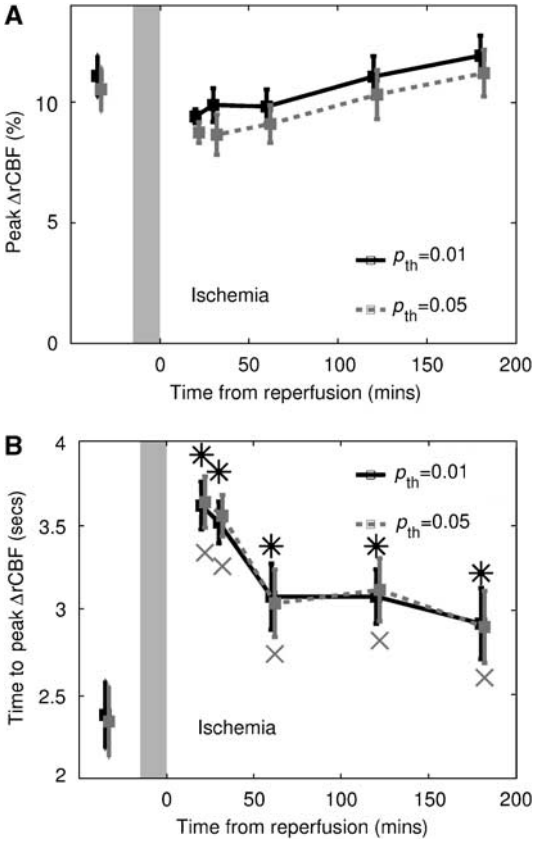

Figure 6 (**A**) Peak ΔrCBF response before and after ischemic insult ($N = 10$). Peak ΔrCBF response to the stimulation was not significantly influenced by the ischemic insult ($P = 0.14$ and 0.18 for $p_{th} = 0.01$ and 0.05, respectively). (**B**) Time to peak ΔrCBF response increased significantly after reperfusion ($P < 0.0001$ for both thresholds) and recovered slowly toward the preischemic value ($N = 10$). Symbols indicate significant difference from preischemic values ($P < 0.05$). rCBF, relative cerebral blood flow.

Time to maximum ΔrCBF: Although maximum ΔrCBF was largely unchanged, there was a significant delay in the response to vibrissae stimulation after incomplete ischemia (ANOVA, $P<0.0001$ for both thresholds). As shown in Figure 6B, the time to peak response increased from 2.4 ± 0.2 secs before forebrain ischemia to 3.6 ± 0.1 secs approximately 20 mins into reperfusion ($P=0.0006$). The time delay slowly recovered toward the preischemic level, for example, 3.5 ± 0.1 secs at 30 mins ($P=0.0005$), 3.1 ± 0.2 secs at 1 h ($P=0.04$), and 3.1 ± 0.2 secs at 2 h ($P=0.03$) into the reperfusion. Even 3 h after reperfusion, the time to peak remained significantly elevated (2.9 ± 0.2 secs, $P=0.04$). The time to peak in the control (sham ischemia) group was stable throughout the study (ANOVA, $P=0.10$).

Discussion

The phenomenon of hypoperfusion and postischemic hyperperfusion has been investigated extensively after severe incomplete ischemia in rat (Kagstrom *et al*, 1983; Inamura *et al*, 1988; Dirnagl *et al*, 1993). Cerebral blood flow measured in the cortex was found to be less than 10% of the preischemic level after 10 to 15 mins of incomplete ischemia (Kagstrom *et al*, 1983; Inamura *et al*, 1988; Dirnagl *et al*, 1993), which is in agreement with our observations. After 5 mins reperfusion, a 250% to 300% hyperemia was usually seen (Kagstrom *et al*, 1983; Dirnagl *et al*, 1993), which is lower than the peak value observed 9 to 10 mins after the end of the ischemia in our study ($538\% \pm 35\%$). These differences might be related to differences in anesthesia or duration of ischemia between the studies. Dunn *et al* (2001) have validated laser speckle against laser Doppler in rat brains over a wide range of rCBF values (from 0% to 250% of baseline). However, to our knowledge, no validation study has been reported at a higher perfusion level. It is possible that laser speckle overestimates blood flow during reperfusion in the current study. Further studies are needed to validate the accuracy of laser speckle technique at high perfusion levels.

It is believed that functional impairment/recovery after stroke depends on the duration and severity of cerebral ischemia. Schmitz *et al* (1998) have shown in rats with 10 mins of cardiac arrest that blood oxygen level-dependent measurement and perfusion responses to forepaw stimulation were impaired 1 h after the cardiac arrest. Blood oxygen level-dependent measurement eventually recovered at 1 day, but at that time, perfusion only recovered to about 50%. In the same animal model, Schmitz *et al* (1997) also showed, using laser Doppler and autoradiography, that blood flow response to forepaw stimulation was completely suppressed at 45 mins. In some but not all animals, a weak response could be observed by 1.5 h, followed by a gradual improvement of 50% to 60% of control within 3 days. Using functional MRI, Shen *et al* (2005) showed that with permanent focal ischemia (middle cerebral artery occlusion), CBF response to the forepaw stimulation in the primary somatosensory cortices was lost, although CO_2 reactivity of the vasculature was intact. After transient (15 mins) ischemia, blood flow response to the forepaw stimulation was normalized by 30 mins and remained unaltered throughout the 24 h of monitoring. It should be noted, however, that this model does not produce permanent damage.

These prior studies investigated the impairment/recovery of amplitude in response to functional challenges (CO_2, electrical forepaw stimulations, and so on). However, less is known about the spatial and temporal recovery of the brain with transient ischemia in response to functional challenges, because of the limited spatial and temporal resolution of most imaging techniques (MRI and PET). In the current study, we exploited the superior spatial and temporal resolution of LSI to address this question. We also used the SPM approach to analyze our laser speckle data, which enabled the comparison of brain activation under different physiologic conditions. The time period (2 to 5 secs into stimulation) used for contrasting was chosen to cover the peak activations. We also tried contrasting different time periods (i.e., 1 to 5 secs, 2 to 6 secs into stimulation) with baseline. Similar trends were observed for the changes in activation area, maximum ΔrCBF, and time to maximum ΔrCBF. In GLM analyses, the hemodynamic response function can also be modeled in a variety of ways to examine significant changes between conditions (Woolrich *et al*, 2004), and it would also be possible to test complex models with various contrasts and covariates, including covariates for ischemic states, so as to generate maps showing regions of significant change at different states. These approaches will be explored in future laser speckle studies.

In SPM, variations of resting rCBF within 5 secs before stimulation were taken into account for the statistical analysis. Pixels within ROIs defined by a statistical threshold (e.g., $p_{th}=0.01$) have rCBF changes well above the baseline noise level and are therefore considered to be reliably activated. However, the same rCBF change because of functional stimulation may show a larger or smaller activation area if the variability of resting rCBF is influenced by the ischemic insult. To check the potential influence of this possibility on our conclusion, we have employed constant ΔrCBF thresholds (4%, 5%, and 7%) for the definition of ROIs before and after the ischemic insult. Consistent activation area changes were observed compared with the *t*-threshold results shown above (Figure 4). In addition, variations of resting rCBF were analyzed and found unchanged before and after ischemia (ANOVA, $P=0.99$). Therefore, the influence of resting rCBF variability on the spatial extent of activation is minimal in our study.

We have employed a variable ROI before and after ischemia for the analysis of ΔrCBF response to

vibrissae stimulation. Another approach is to use a fixed ROI determined by SPM before the ischemic insult for analysis at all the time points. In this case, peak ΔrCBF showed a significant decrease after ischemia and subsequently recovered (Figure 7A), although the time to peak ΔrCBF (Figure 7B) followed a trend similar to that observed in Figure 6B. The difference in peak ΔrCBF before and after ischemia was less significant when a variable ROI was used (Figure 6A). Note, however, that the peak ΔrCBF response in Figure 7A followed the same trend as the activation area changes with a variable ROI (Figure 4). The different peak ΔrCBF response between a fixed ROI and a variable ROI is probably because of the inclusion of pixels that are less activated after ischemia. The approach of using a fixed ROI, therefore, cannot separate the ischemia influence on the temporal and spatial response of ΔrCBF.

In a nonischemic rat, the spatial extent of hemodynamic changes (oxy, deoxy, and total hemoglobin concentrations and CBF) in response to whisker stimulation is usually larger than the size of the whisker barrels (Devor *et al*, 2003; Weber *et al*, 2004; Dunn *et al*, 2005). In the current study, the activation area observed before ischemia agrees well with the literature, considering that the distance between adjacent whisker barrels is about 400 to 500 μm (Masino *et al*, 1993), and the CBF response is less localized compared with hemoglobin changes (Dunn *et al*, 2003) and oxidative metabolism (Weber *et al*, 2004). One of our principle findings is that the activation area in response to functional stimulation is significantly reduced after the ischemic insult. However, baseline blood flow was found to recover 1 h after the reperfusion, and we observed a sign of recovery in the activation area at the 2 h time point. This phenomenon was quite robust and was consistent among all animals, which may suggest the existence of a window for functional recovery. It should be noted that the principal parameter of measurement in this study was blood flow (obtained with speckle contrast) and that alterations in the hemodynamic response may not be necessarily because of alterations in the ability of the vasculature to respond. There is evidence that evoked responses may be altered early after cerebral ischemia (Schmitz *et al*, 1997), raising the possibility that the observed changes may not be solely because of changes in activation flow coupling. In a recent study (Burnett *et al*, 2005), however, CBF measured with laser Doppler was found correlated with the amplitude of the somatosensory evoked potentials during ischemia, suggesting that CBF reflects neural function. Further studies correlating CBF and neural function would be needed to determine the basis for the observed hemodynamic changes.

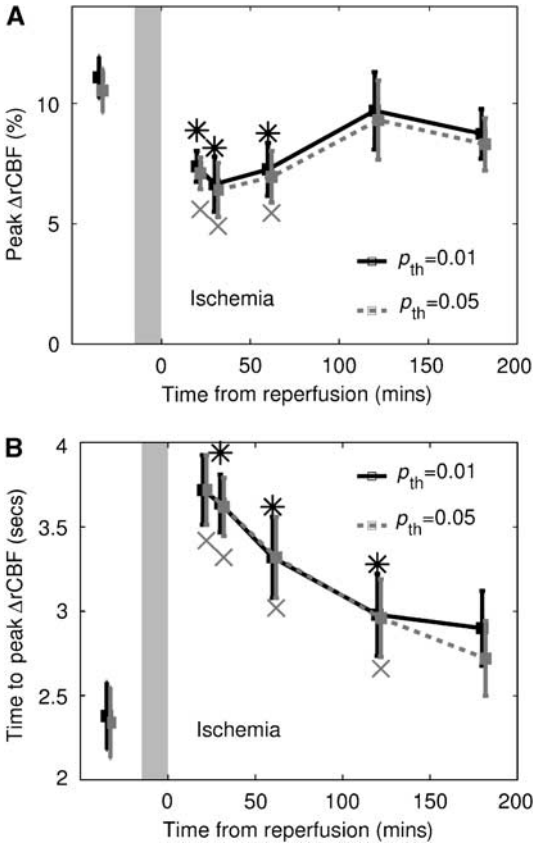

Figure 7 Peak ΔrCBF (**A**) and time to peak ΔrCBF (**B**) responses before and after ischemic insult ($N = 10$) using a fixed preischemic region of interest ($p_{th} = 0.01$ and 0.05, respectively). Symbols indicate significant difference from preischemic values ($P < 0.05$). rCBF, relative cerebral blood flow.

Another major effect of the ischemic insult was the variations in the temporal profile of rCBF in response to stimulation. Before ischemia, rCBF started increasing about 1 sec after the onset of the stimulation and took 2.4 ± 0.2 secs to peak, in line with the previously observed hemodynamic changes during both forepaw (Ances *et al*, 2001; Durduran *et al*, 2004; Dunn *et al*, 2005) and whisker (Jones *et al*, 2001; Dunn *et al*, 2003, 2005; Weber *et al*, 2004) stimulations in the rat. Note that the temporal profile of the rCBF response was averaged over the whole activation area, with the maximum ΔrCBF response reflecting an average change of the activated region. The peak response of $11.1\% \pm 0.9\%$ from the nine-whisker stimulation is thus comparable with the results from single-whisker stimulations (Dunn *et al*, 2003, 2005; Weber *et al*, 2004), although less than what was seen in layer IV of the cortex using autoradiography (Greenberg *et al*, 1999). After the ischemic insult, significant delay of the time to peak ΔrCBF was observed and this delay gradually returned toward normal (Figure 6B). It is interesting to note that the peak ΔrCBF was not significantly influenced by the ischemic insult. To the extent that CBF changes reflect underlying neural metabolism, this may suggest that in the early stages of reperfusion, the somatosensory cortex 'worked as hard as' before ischemia, but the vasculature responded more slowly to the stimulation. We

previously observed a prolonged time to peak after unilateral carotid occlusion and attributed the delay to the use of a circuitous recruitment of collateral supply (Ances *et al*, 2000). However, in the present study, the carotids were reopened, suggesting that the observed delay may represent an alteration in activation flow coupling after the ischemic insult.

Conclusions

We have incorporated the SPM method into LSI to investigate functional spatial and temporal responses of CBF after temporary incomplete cerebral ischemia in the rat. Modified GLM and SPM offer robust statistical parametric maps and enable the comparison of activation under various physiologic conditions. Our results show that the ischemic insult significantly alters CBF, the area of activation, and the temporal response to stimulation. The magnitude of the CBF response to functional stimulation, however, was preserved in the early hours after transient incomplete ischemic insult.

Acknowledgements

The authors thank Meeri N Kim for useful discussions.

References

Ances BM, Greenberg JH, Detre JA (2000) Acute carotid occlusion alters the activation flow coupling response to forepaw stimulation in a rat model. *Stroke* 31:955–60

Ances BM, Wilson DF, Greenberg JH, Detre JA (2001) Dynamic changes in cerebral blood flow, O_2 tension, and calculated cerebral metabolic rate of O_2 during functional activation using oxygen phosphorescence quenching. *J Cereb Blood Flow Metab* 21:511–6

Ayata C, Dunn AK, Gursoy-Ozdemir Y, Huang ZH, Boas DA, Moskowitz MA (2004) Laser speckle flowmetry for the study of cerebrovascular physiology in normal and ischemic mouse cortex. *J Cereb Blood Flow Metab* 24: 744–55

Bandyopadhyay R, Gittings AS, Suh SS, Dixon PK, Durian DJ (2005) Speckle-visibility spectroscopy: a tool to study time-varying dynamics. *Rev Sci Instru* 76:093110

Benzi G, Dagani F, Arrigoni E (1978) Acute model for the estimation of the cerebral energy state during or after hypoxia and complete or incomplete ischaemia. *Eur Neurol* 17:87–96

Boas DA, Yodh AG (1997) Spatially varying dynamical properties of turbid media probed with diffusing temporal light correlation. *J Opt Soc Am A Opt Image Sci Vis* 14:192–215

Bonner RF, Nossal R (1990) Principles of laser-Doppler flowmetry. In: *Laser-Doppler Blood Flowmetry* (Shepherd AP, Oberg PA, eds), Boston: Kluwer Academic Publishers, 17–45

Bookstein FL (1989) Principal warps—thin-plate splines and the decomposition of deformations. *IEEE Trans Pattern Anal Mach Intell* 11:567–85

Briers JD (2001) Laser Doppler, speckle and related techniques for blood perfusion mapping and imaging. *Physiol Meas* 22:R35–66

Burnett MG, Detre JA, Greenberg JH (2005) Activation-flow coupling during graded cerebral ischemia. *Brain Res* 1047:112–8

Devor A, Dunn AK, Andermann ML, Ulbert I, Boas DA, Dale AM (2003) Coupling of total hemoglobin concentration, oxygenation, and neural activity in rat somatosensory cortex. *Neuron* 39:353–9

Dietrich WD, Busto R, Yoshida S, Ginsberg MD (1987) Histopathological and hemodynamic consequences of complete versus incomplete ischemia in the rat. *J Cereb Blood Flow Metab* 7:300–8

Dijkhuizen RM, Singhal AB, Mandeville JB, Wu O, Halpern EF, Finklestein SP, Rosen BR, Lo EH (2003) Correlation between brain reorganization, ischemic damage, and neurologic status after transient focal cerebral ischemia in rats: a functional magnetic resonance imaging study. *J Neurosci* 23:510–7

Dirnagl U, Thoren P, Villringer A, Sixt G, Them A, Einhaupl KM (1993) Global forebrain ischemia in the rat: controlled reduction of cerebral blood flow by hypobaric hypotension and two-vessel occlusion. *Neurol Res* 15:128–30

Dunn AK, Bolay H, Moskowitz MA, Boas DA (2001) Dynamic imaging of cerebral blood flow using laser speckle. *J Cereb Blood Flow Metab* 21:195–201

Dunn AK, Devor A, Bolay H, Andermann ML, Moskowitz MA, Dale AM, Boas DA (2003) Simultaneous imaging of total cerebral hemoglobin concentration, oxygenation, and blood flow during functional activation. *Opt Lett* 28:28–30

Dunn AK, Devor A, Dale AM, Boas DA (2005) Spatial extent of oxygen metabolism and hemodynamic changes during functional activation of the rat somatosensory cortex. *Neuroimage* 27:279–90

Durduran T, Burnett MG, Yu GQ, Zhou C, Furuya D, Yodh AG, Detre JA, Greenberg JH (2004) Spatiotemporal quantification of cerebral blood flow during functional activation in rat somatosensory cortex using laser-speckle flowmetry. *J Cereb Blood Flow Metab* 24: 518–25

Friston KJ, Holmes AP, Worsley KJ, Poline JB, Frith CD, Frackowiak RS (1995) Statistical parametric maps in functional imaging: a general linear approach. *Hum Brain Map* 2:189–210

Goodman J (1985) *Statistical Optics*. John Wiley & Sons: Hoboken, NJ

Greenberg JH, Sohn NW, Hand PJ (1999) Nitric oxide and the cerebral-blood-flow response to somatosensory activation following deafferentation. *Exp Brain Res* 129: 541–50

Inamura K, Smith ML, Olsson Y, Siesjö BK (1988) Pathogenesis of substantia nigra lesions following hyperglycemic ischemia: changes in energy metabolites, cerebral blood flow, and morphology of pars reticulata in a rat model of ischemia. *J Cereb Blood Flow Metab* 8:375–84

Jones M, Berwick J, Johnston D, Mayhew J (2001) Concurrent optical imaging spectroscopy and laser-Doppler flowmetry: the relationship between blood flow, oxygenation, and volume in rodent barrel cortex. *Neuroimage* 13:1002–15

Kagstrom E, Smith ML, Siesjo BK (1983) Recirculation in the rat-brain following incomplete ischemia. *J Cereb Blood Flow Metab* 3:183–92

Kernick DP, Tooke JE, Shore AC (1999) The biological zero signal in laser Doppler fluximetry—origins and practical implications. *Pflugers Arch* 437:624–31

Masino SA, Kwon MC, Dory Y, Frostig RD (1993) Characterization of functional organization within rat barrel cortex using intrinsic signal optical imaging through a thinned skull. *Proc Natl Acad Sci USA* 90:9998–10002

Nordström CH, Siesjö BK (1978) Effects of phenobarbital in cerebral ischemia. Part I: cerebral energy metabolism during pronounced incomplete ischemia. *Stroke* 9: 327–35

Schmitz B, Bock C, Hoehn-Berlage M, Kerskens CM, Böttiger BW, Hossmann KA (1998) Recovery of the rodent brain after cardiac arrest: a functional MRI study. *Magn Reson Med* 39:783–8

Schmitz B, Bottiger BW, Hossmann KA (1997) Functional activation of cerebral blood flow after cardiac arrest in rat. *J Cereb Blood Flow Metab* 17:1202–9

Shen Q, Ren H, Cheng H, Fisher M, Duong T (2005) Functional, perfusion and diffusion MRI of acute focal ischemic brain injury. *J Cereb Blood Flow Metab* 25:1265–79

Shin HK, Dunn AK, Jones PB, Boas DA, Moskowitz MA, Ayata C (2006) Vasoconstrictive neurovascular coupling during focal ischemic depolarizations. *J Cereb Blood Flow Metab* 26:1018–30

Smith ML, Bendek G, Dahlgren N, Rosén I, Wieloch T, Siesjö BK (1984) Models for studying long-term recovery following forebrain ischemia in the rat. 2. A 2-vessel occlusion model. *Acta Neurol Scand* 69:385–401

Sohn NW, Greenberg JH, Hand PJ (1999) Chronic inhibition of NOS does not prevent plasticity of rat somatosensory (s1) cortex following deafferentation. *Brain Res* 816:396–404

Steen PA, Michenfelder JD, Milde JH (1979) Incomplete versus complete cerebral ischemia: improved outcome with a minimal blood flow. *Ann Neurol* 6:389–98

Strong A, Bezzina E, Anderson P, Boutelle M, Hopwood S, Dunn A (2006) Evaluation of laser speckle flowmetry for imaging cortical perfusion in experimental stroke studies: quantitation of perfusion and detection of peri-infarct depolarisations. *J Cereb Blood Flow Metab* 26: 645–53

Ueki M, Linn F, Hossmann KA (1988) Functional activation of cerebral blood flow and metabolism before and after global ischemia of rat brain. *J Cereb Blood Flow Metab* 8:486–94

Wang Z, Hughes S, Dayasundara S, Menon R (2007) Theoretical and experimental optimization of laser speckle contrast imaging for high specificity to brain microcirculation. *J Cereb Blood Flow Metab* 27:258–69

Weber B, Burger C, Wyss MT, von Schulthess GK, Scheffold F, Buck A (2004) Optical imaging of the spatiotemporal dynamics of cerebral blood flow and oxidative metabolism in the rat barrel cortex. *Eur J Neurosci* 20:2664–70

Woolrich M, Behrens T, Smith S (2004) Constrained linear basis sets for HRF modelling using Variational Bayes. *Neuroimage* 21:1748–61

Worsley KJ, Friston KJ (1995) Analysis of fMRI time-series revisited-again. *Neuroimage* 2:173–81